9-2006

Mapped Overland Distance of Paleotsunami High-Velocity Inundation n Back-Barrier Wetlands of the Central Cascadia Margin, U.S.A

Robert B. Schlichting
Portland State University

Curt D. Peterson
Portland State University

Citation Details

Schlichting, R. B., & Peterson, C. D. (2006). Mapped Overland Distance of Paleotsunami High-Velocity Inundation n Back-Barrier Wetlands of the Central Cascadia Margin, U.S.A. Journal of Geology, 114(5), 577-592.

Mapped Overland Distance of Paleotsunami High-Velocity Inundation in Back-Barrier Wetlands of the Central Cascadia Margin, U.S.A.

Robert B. Schlichting and Curt D. Peterson

Geology Department, Portland State University, Portland, Oregon 97207-0751, U.S.A.
(e-mail: rbs@integraonline.com)

ABSTRACT

Investigations of back-barrier, open-coastal plain settings have been used to establish minimum inundation distances of prehistoric tsunamis produced by great subduction zone earthquakes in the central Cascadia margin. Distinctive sand sheets were characterized at four localities within the central Cascadia margin, a shoreline distance of about 250 km. The sand sheets vary in thickness from 0.2 to 25 cm. They thin in the landward direction and consist of well-sorted beach sand that fines upsection. Many of the sand sheets include capping layers of organic-rich detritus, as well as assimilated mud rip-up clasts and soil litter. Marine diatoms and bromine (i.e., marine tracers) were used to confirm marine surge origins for the anomalous sand sheets. Radiocarbon dating of the sand sheets demonstrates correspondence with reported great Cascadia earthquake events at 0.3, ~1.1, ~1.3, ~1.7, and ~2.5 Ka. One sand sheet mapped at all four localities is dated at 600–950 calibrated radiocarbon years before present. This interpreted paleotsunami event does not correspond to a central Cascadia rupture, so it is tentatively assigned to a far-field source. Minimum overland inundation distances of the near field (Cascadia tsunami) at the four study localities range from 0.3 to 1.3 km, with a mean inundation for all sand sheets of 0.5 km.

Introduction

Shorelines bordering the northeast Pacific Ocean (fig. 1) are subject to near-field tsunamis, which originate from great earthquakes in the adjacent Cascadia subduction zone (Darienzo and Peterson 1990; Clague and Bobrowsky 1994). The last Cascadia earthquake that produced a tsunami occurred in 1700, as demonstrated by geologic records in coastal deposits (Atwater et al. 1995) and historic tsunami run-up records in Japan (Satake et al. 1996). A lack of modern tsunamis in the Cascadia margin has led to uncertainty about potential inundation hazards for this coastline (Priest 1995). Excitation and propagation modeling for tsunamis originating in the central Cascadia margin has constrained evacuation time (15–30 min) following fault rupture (Myers et al. 1999). However, modeled inundation distances are dependent on unverified excitation parameters (Priest et al. 2000).

Paleotsunami records, such as sand sheet deposition, provide evidence of high-velocity inundation, as observed from modern tsunamis in other margins (Jaffe and Gelfenbaum 1998). To date, most of the reported paleotsunami deposits in the Cascadia margin are from coseismically subsided wetlands in tidal basins (Peters et al. 2003). Interpretations of paleotsunami magnitude from tidal basin deposits are complicated by the tidal basin bathymetry and hydrographics. These complications include channel hydrodynamics, coincident tidal stages, and basin seiches (Myers et al. 1999). By comparison, paleotsunami sand deposits that are preserved in peat bogs from low-elevation beach plains (Schlichting 2000) provide less complicated evidence of surge inundation distance.

In this article, we use geologic records of paleotsunamis to establish potential tsunami hazard on the open coast in the central Cascadia margin. Paleotsunami sand sheets were mapped in four localities to establish the potential for near-field tsunamis to inundate open-coastal areas where surge dynamics are not influenced by bay inlets, tidal flats, or channels. Paleotsunami deposits have been characterized, correlated, and traced inland by shallow coring, grain size analyses, diatom analyses, bromine analyses, and radiocarbon dating. The re-

Manuscript received February 8, 2005; accepted March 5, 2006.

[The Journal of Geology, 2006, volume 114, p. 577–592] 0022-1376/2006/11405-0004$15.00

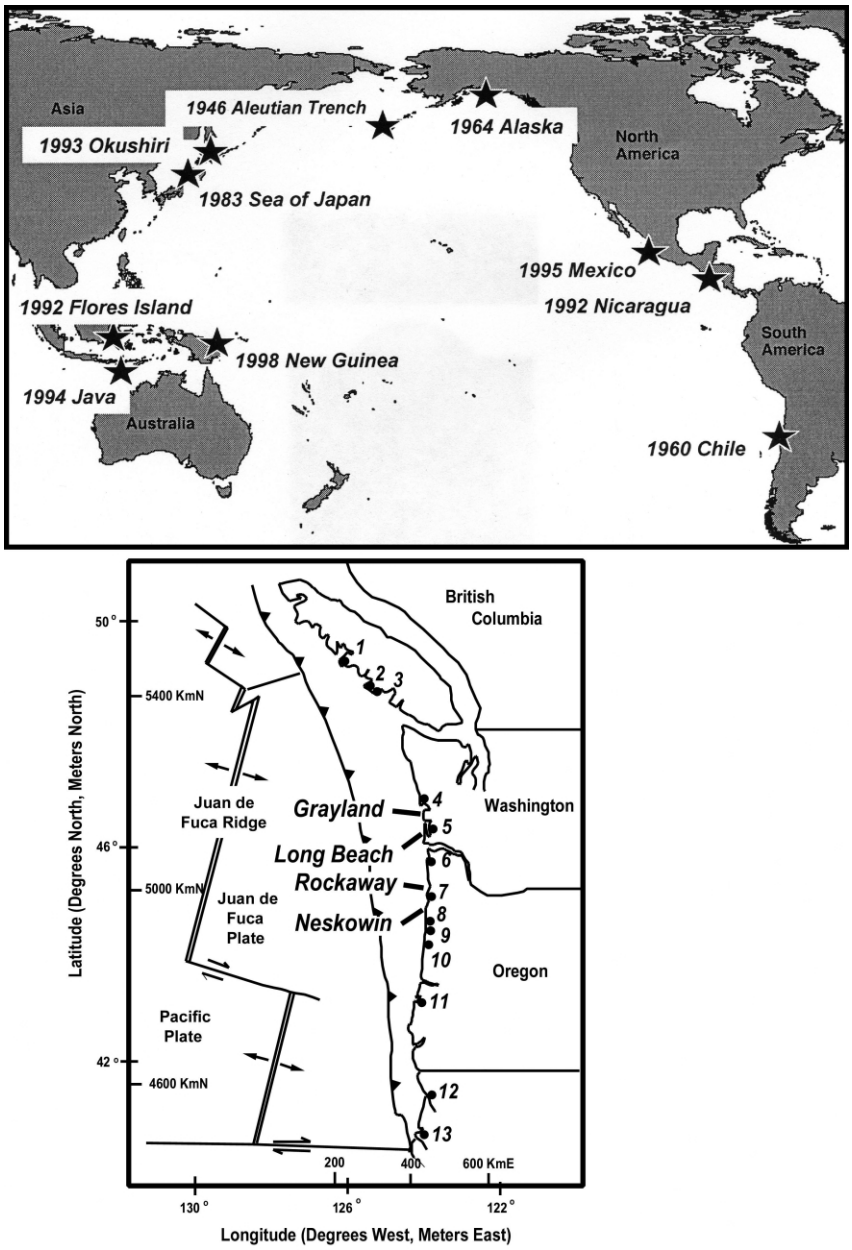

Figure 1. All of the major convergent plate margins along the Pacific Basin margin except the Cascadia margin have examples of devastating tsunamis within the past half century. However, a number of tidally influenced sites along the Pacific coast show evidence of tsunami inundation within the Cascadia margin. These include (*1*) Kanim Lake, (*2*) Tofino, (*3*) Port Alberni, (*4*) Copalis River, (*5*) Willapa River, (*6*) Seaside, (*7*) Netarts Bay, (*8*) Siletz Bay, (*9*) Alsea Bay, (*10*) Yaquina Bay, (*11*) Coos Bay, (*12*) Lagoon Creek, and (*13*) Humboldt Bay. Triangles indicate the open-coastal freshwater wetland sites investigated for this article.

sulting data are used to predict high-velocity inundation distances for a variety of coastal plain localities in the central Cascadia margin.

Background

The turbulent nature of tsunami inundation (Minoura et al. 1994) induces sediment entrainment near shorelines and deposition at inland sites under waning flow velocities. The turbulent suspension and transport of fine to medium-size sand for large distances (hundreds of meters) over vegetated terrain requires high-velocity flow (>1 m s^{-1}). The preservation of fining-up beach sand layers hosted in peat or lagoonal mud layers permits the mapping

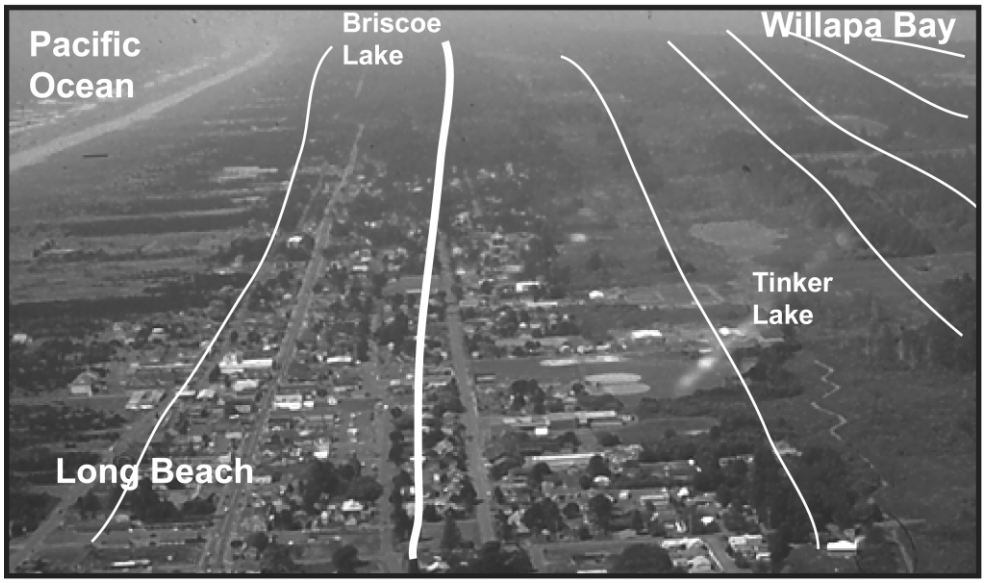

Figure 2. Aerial photograph of the Long Beach Peninsula, southwest Washington. The approximate crests of the dune ridges are shown by white lines. The presence of trees on the ridges indicates the accelerated rate of soil development on these upland areas. Interdune lows are occupied by lakes and bogs. Deposits located in these interdune areas were the focus of this study.

of paleotsunami inundation distance (Foster 1991). Soil litter, organic detritus, and mud rip-ups are also entrained by high-velocity tsunami inundation. These materials are frequently interbedded with sand layers during deposition under waning conditions of tsunami wave trains.

In the central Cascadia margin, paleotsunami deposits are well documented from tidal wetland settings, where they occur as fining-up sand layers hosted in peaty mud deposits (Atwater 1987, 1992; Darienzo and Peterson 1990; Clague and Bobrowsky 1994; Peterson and Priest 1995). Paleotsunami sand sheets are also well preserved in freshwater ponds (Nelson et al. 1996; Clague et al. 1999). In such freshwater settings, the presence of marine diatoms in the anomalous sand layers provides additional evidence of marine surge inundation (Hutchinson et al. 1997). Paleotsunami deposits in tidal basins, lagoons, and ponds have been well documented. Yet it was not known whether overland inundation would leave unambiguous tsunami deposits preserved in the geologic record.

Field Locality Settings

Four localities in the central Cascadia margin were investigated for prehistoric tsunamis. These localities are Neskowin and Rockaway, Oregon, and Long Beach Peninsula and Grayland Plains, Washington (fig. 1). These localities are situated on prograded beach plains or barrier spits with relatively straight shorelines and low back-barrier elevations relative to mean sea level (MSL; fig. 2). Bogs and ponds are interspersed on the beach plains (3–5 m above MSL) landward of foredune ridges (6–10 m above MSL). The natural bogs are currently vegetated by *Carex* sp. and shrub willow (~1 m in height). Stabilized foredunes are rapidly forested by spruce, fir, and shore pine. The distribution of study sites was chosen to test local variability of inundation between paired localities (~50 km separation) and regional variability of inundation between the Oregon and Washington localities (200 km maximum separation). Preliminary field examinations demonstrated high preservation potential for thin sand sheets deposited in the back-barrier bogs of the four study localities (Schlichting 2000).

The two Oregon localities (Neskowin and Rockaway) consist of bogs and ponds that developed landward of continuous sand barriers (0.3–0.5 km in width) that stabilized in their present positions at least 2000 yr ago (Hart and Peterson 1997). By comparison, the Washington localities (Long Beach and Grayland) have a history of episodic shoreline progradation (net average accretion of 0.5 m yr^{-1}) for the last 2000 yr (Peterson et al. 1999). The net progradation, forced by excess sand supply from the

Columbia River, is interrupted by catastrophic beach retreat resulting from coseismic subsidence every few hundred years (Meyers et al. 1996). The beach retreat events have been mapped, radiocarbon dated, and correlated to earthquake events, yielding dated shoreline positions (Woxell 1998). Preretreat shoreline positions are estimated to have existed 100–300 m seaward of the retreat scarps during corresponding Cascadia tsunami inundation (Doyle 1996).

Methods

Buried sand and detritus layers hosted in mud or peat deposits were analyzed from about 200 sites at the four study localities in northwest Oregon and southwest Washington between 1997 and 2000 (fig. 1). Reconnaissance coring for wetland stratigraphy (0.5–4 m subsurface depth) was performed with a gouge core (2.5 cm in diameter). Cores were logged to the nearest centimeter for lithology (mud, peat, sand), sand grain size, and detritus materials. Vibracores (7 cm in diameter) were used to collect uncontaminated, continuous cores for radiocarbon dating, diatom analyses, and geochemical analyses of bromine (fig. 3). Core sites were georeferenced with the differential Global Positioning System (EPE ± 10 m, WSG84).

Target tsunami sand deposits were visually examined for beach sand lithology and grain rounding by hand lens and for mean grain size by grain size card. Paleotsunami sand layers from two core transects at Neskowin were subsectioned and sampled for sieve analysis of sand grain size distribution at one-quarter Φ size intervals (Folk 1980). The quantitative grain size analyses were employed to test for the presence of fining-up sequences and fining-inland trends that could result from waning turbulent suspension in landward-directed transport.

Two stratigraphic cores from Briscoe Lake, Long Beach Peninsula, Washington, were subsampled downcore (1-cm intervals) for analysis of diatoms and geochemical markers, for example, Br, Na, and K (Schlichting 2000). The geochemical marker bromine is of particular interest because it is found in marine water but not in terrestrial sources (Duce et al. 1965; Fuge 1988). Diatom sample preparation and counting follow Darienzo (1987), Hemphill-Haley (1996), and Hutchinson et al. (1997). Diatom assemblages were quantified by counting the total number of diatoms (valves) from 10 randomly positioned microscope fields of view for each sample. The number of marine diatoms per slide was also counted to yield the marine diatom fraction for each sample.

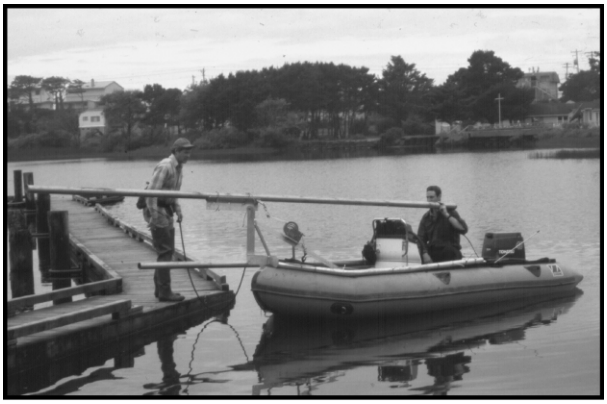

Figure 3. Aluminum pipes were penetrated into sediments using a vibracore that had been mounted onto the front of a boat.

The downcore presence and concentration of marine geochemical markers was evaluated using neutron activation analysis. The elements of interest included bromine, sodium, and potassium. In addition, a number of rare earth and trace elements were included in the analysis. Subsamples of core material were dried, pulverized, and massed before analysis. Samples were irradiated for 1 h with a neutron flux of 2×10^{12} neutrons cm^{-2} s^{-1} at the Reed College nuclear reactor, Portland, Oregon. Irradiated samples were quantified using a germanium crystal gamma-ray spectrometer. Standard reference tables were calibrated using coal fly ash and potassium bromide standards.

Materials selected for radiocarbon dating included twigs, conifer needles, and bulk peat samples. The twigs and conifer needles were extracted from target tsunami sand layers or detrital caps and were dated by the AMS radiocarbon method. Bulk peat samples were collected from peat intervals between target tsunami layers and from basal peat deposits to constrain the ages of the hosting deposits. All radiocarbon samples were handpicked to remove descending roots, rinsed in deionized water, and dried before submittal to Beta Analytic. Radiocarbon ages are presented as calibrated radiocarbon years before present (cal. RYBP) based on calibration curves of Stuiver and Reimer (1993).

Results

Paleotsunami Core Transects. The numbers of target tsunami deposits, that is, sand layers hosted in

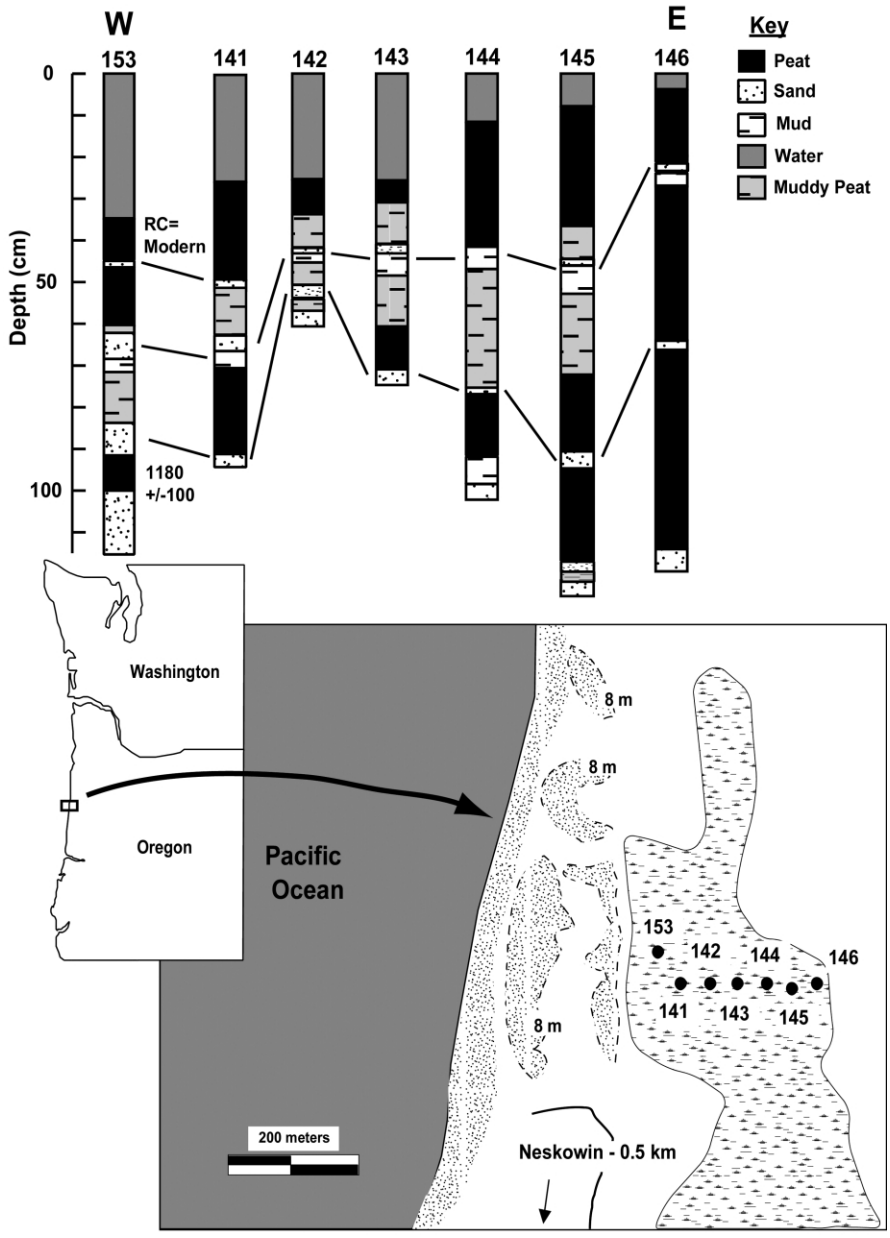

Figure 4. Inland-oriented core transect from the marsh located north of Neskowin, Oregon. *RC* = radiocarbon years before present.

mud or peat, from individual core sites range from one (all site locations) to seven at Crescent Lake, Rockaway (fig. 8). Only the four youngest (i.e., shallowest) sand sheets are discussed in this article. Core transects from Neskowin and Rockaway, Oregon, and Long Beach and Grayland, Washington, are shown in figures 4–7. Target tsunami deposits are correlated between core sites based on the number, depth, and sequence of distinct sand layers. The lateral extent of continuous tsunami layers, that is, stratigraphically correlated sand sheets, ranged from 0.2 to 0.80 km in landward distance. In summary, target tsunami layers were observed in 100% of the cores from Neskowin and Rockaway, 100% of the cores from Grayland Plains, and 30% of the cores from Long Beach Peninsula. Only the Long Beach locality had sufficiently wide hosting environments (2 km wide) to extend beyond the distance of observed sand transport from the larger paleotsunamis. The inundation distances

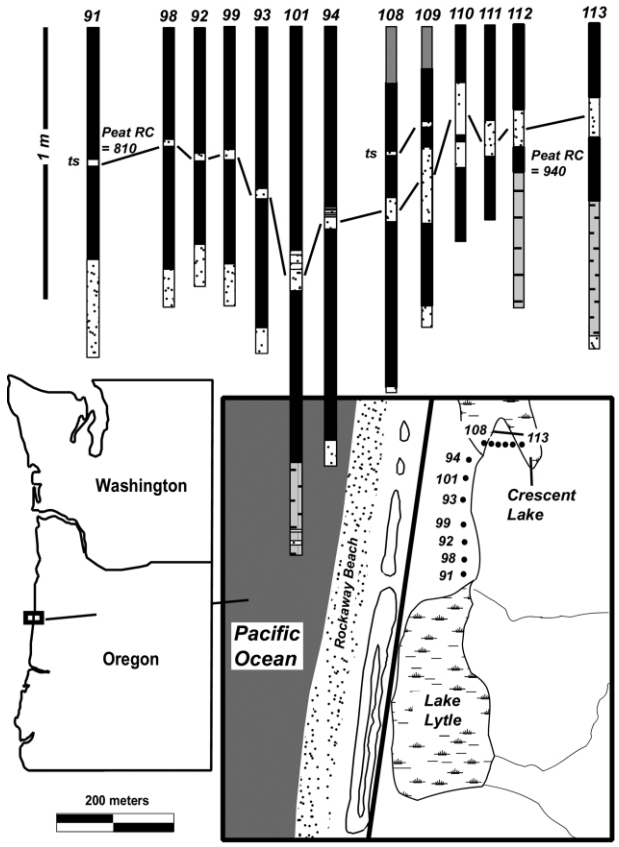

Figure 5. Core transect, Rockaway, Oregon. *RC* = radiocarbon years before present; *ts* = tsunami sand layer.

for the largest Cascadia tsunamis reported for Grayland Plains, Rockaway, and Neskowin are limited by the landward extent of suitable hosting environments, that is, wetland peat or lagoonal mud. Therefore, the inundation distances reported here represent minimum estimates of actual sand transport.

Criteria for Identifying Paleotsunami Deposits. The criteria by which the target sand layers were inferred to be of high-velocity marine surge origin, and specifically of tsunami origin, are summarized in table 1. A sand layer was considered to be of marine origin (criteria 1–2) if it displayed marine markers, such as beach sand, marine diatoms, and/or elevated bromine concentration. The sand deposit was considered to be the result of high-velocity landward-directed surges if it displayed criteria 3–6, which include decreasing sand deposit thickness and decreasing clast size with increasing distance landward. The most restrictive criteria (criteria 7–11) were used to discriminate tsunamis from storm surges on this northeast Pacific coast. These most restrictive criteria include landward sand transport of at least 500 m (storm surges do not transport sand this far inland), event correlation over tens of kilometers of length scales, and radiocarbon ages consistent with dated Cascadia earthquakes, among others. At least two of the most restrictive criteria (7–11) were required in order to infer a tsunamigenic origin for a corresponding sand sheet.

Characteristics of Paleotsunami Sand Layers. Inferred tsunami sand layers range in thickness from 0.2 to 45 cm. They are composed of fine-upper to medium-upper beach sand grains (mean diameter 0.17–0.50 mm) that are rounded to well rounded and rich in monolithic quartz or feldspar. In addition, organic-rich terrestrial detritus was observed to overlie many of the sand layers (fig. 8). Detritus layers were also observed in cores as distinct units without sand. The target sand layers in the core for Neskowin in figure 5 displayed criteria 1, 3, 4, 6, 7, 8, and 9 from table 1. The sand layers for the Long Beach cores in figure 7 displayed criteria 1, 3, 6, 7, 8, and 9 from table 1. Hence, these example target layers are of inferred tsunami origin.

Paleotsunami beds 3–45 cm in thickness generally displayed multiple fining-up sequences of sand layers (fig. 8). Many of these layers rest conformably upon sharp contacts with underlying peat and mud. Layers of mud and terrestrial, organic-rich detritus lay atop many of the tsunami sand deposits (i.e., debris caps). The upper contact of the tsunami-deposited sand/detritus layers typically grade upward into burial deposits that consist of mud and/or peat. Laminae of terrestrial detritus, mud, and mud rip-up clasts were observed between sand layers in the paleotsunami beds. It is not known whether the sand-detritus couplets represent successive tsunami waves or chaotic surges during a single inundation cycle.

Paleotsunami laminae (0.2–2 cm thick) contain one or more sand laminae (0.2–0.4 cm) that display sharp, though irregular, contacts with underlying peat- and mud-hosting sediments (fig. 8). Detritus laminae (0.2–1.0 mm) consist of a mixture of wood fragments, twigs, conifer needles, blades of grass, spruce bark scales, conifer cones, and fine-grained inorganic material such as mud and silt. Unlike the matted or felted peat deposits, the distinctive detritus caps are typically loose and granular in texture. The abundance of twigs, cones, and needles in the detrital caps indicates that advancing tsunamis inundated forested foredune ridges before flooding the more distal bog and pond settings.

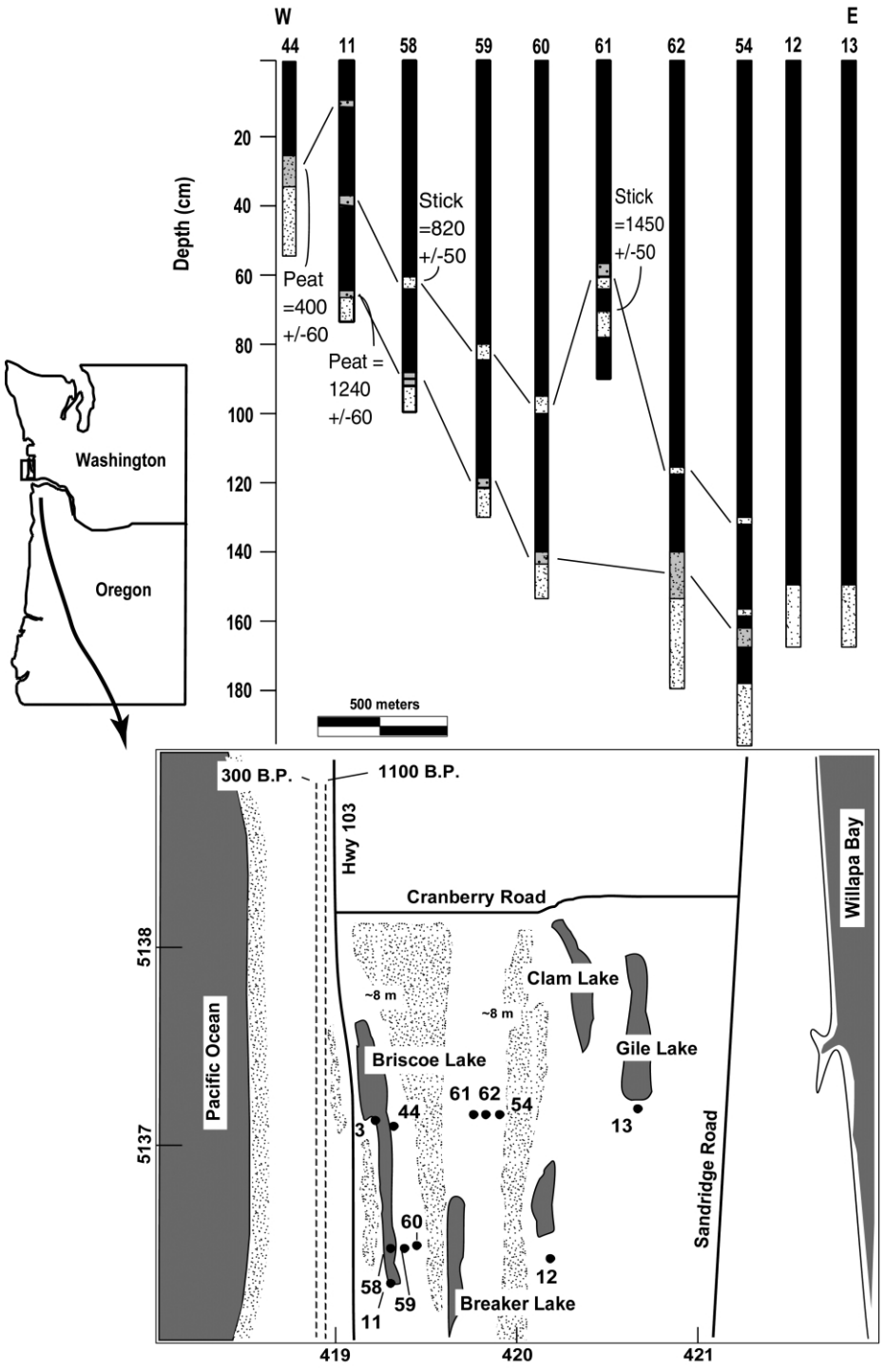

Figure 6. Select core logs from a transect across the central Long Beach Peninsula. The map provides locations of cores, subsurface erosional scarps (Meyers et al. 1996), and current dune elevations.

Quantitative Grain Size Analysis, Neskowin, Oregon. Grain size analyses for selected tsunami sand samples from Neskowin are presented in figure 9. A sand layer at a depth of 63–74 cm was split into an upper and lower fraction. The upper fraction (63–71 cm) had a mean grain size of 0.221 mm, a median size of 0.22 mm, and a standard deviation of 0.0385 mm. The lower fraction (71–74 cm) had

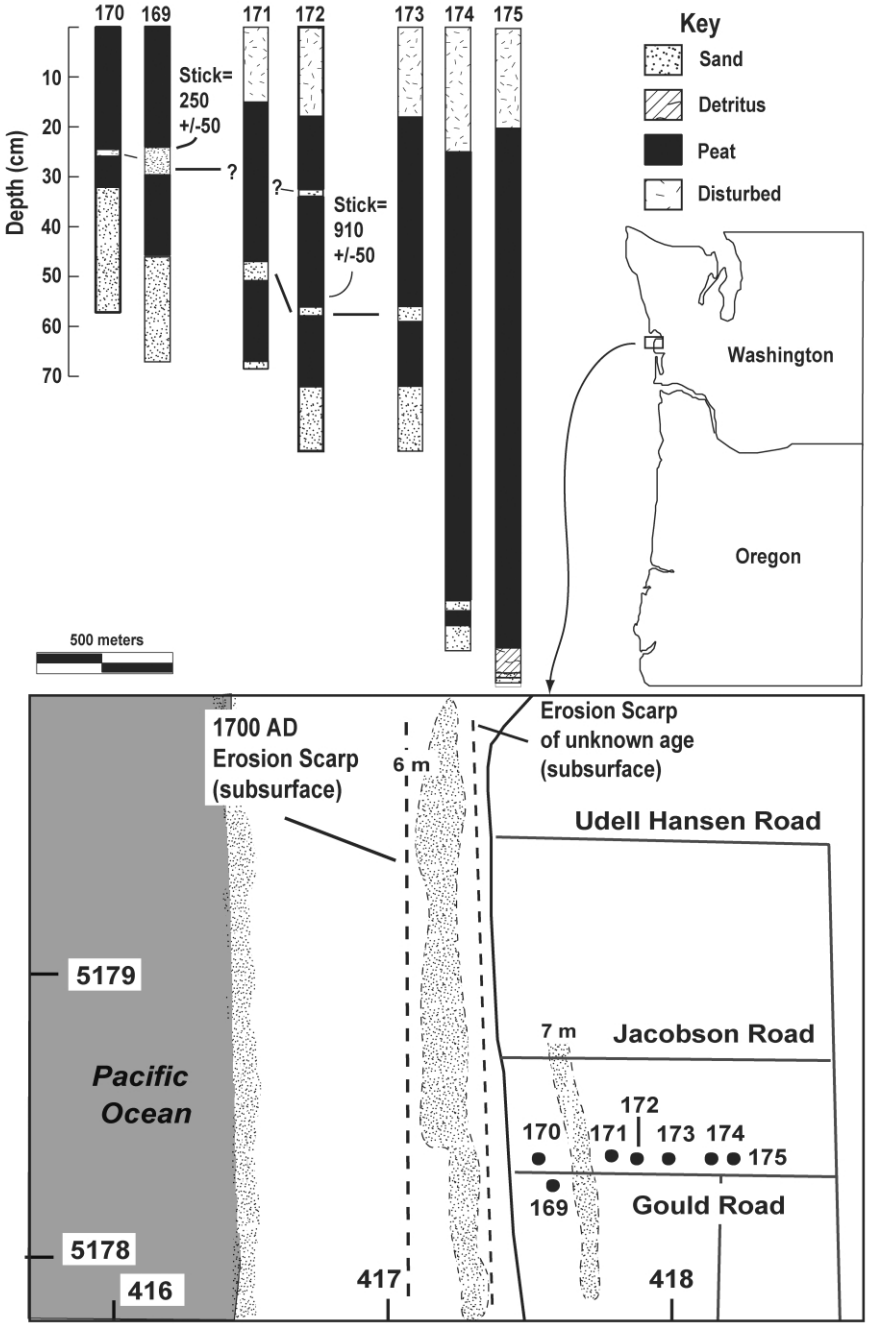

Figure 7. Core logs from a shoreline orthogonal transect for the Grayland Plains central Washington coast.

a mean grain size of 0.239 mm, a median size of 0.239 mm, and a standard deviation of 0.044 mm. Whereas fining-up sequences were noted qualitatively while we cored in the field, these sieving data provide quantitative verification of these observations.

Sand grain size analysis was also performed on correlative sand layers to quantify landward fining of the sand sheets. The sand layer at 63–74 cm below the surface from core 153 returned a mean grain size of 0.233 mm. The correlative sand layer from the landward core located at core site 141 (56–60 cm below surface) had a mean grain size of 0.226 (fig. 9). This limited test proved negative for significant sand size fining over the short distance (300 m) of landward transport between these two

Table 1. Characteristics That Were Used to Distinguish Sand and Terrestrial Derived Detritus Layers as Marine Derived, High- or Low-Velocity Surge Deposited, or Tsunami Deposited

Criterion	Deposit characteristic
1	Clasts are well sorted, quartz rich (derived from beach sand)
2	Deposit shows a marine marker
3	Deposit thickness decreases landward
4	Clast size decreases upsection within deposit
5	Clast size decreases landward
6	Deposit is capped by terrestrial-derived organic material
7	Deposit extends landward over a great distance (>0.5 km)[a]
8	Deposit contains intrasand mud or detritus layers[a]
9	Deposit is broadly correlated locally (within a few kilometers)[a]
10	Deposit is broadly correlated regionally (hundreds of kilometers)[a]
11	Radiocarbon data suggests correlation to a prehistoric Cascadia earthquake event as described in the literature[a]

[a] A deposit was inferred to be tsunami deposited if it exhibited two of characteristics 7–11.

sites. Further, landward sand fining was not observed from descriptive core logs over longer distances (500–1000 m) in other locality transects.

Diatom Analyses from Long Beach, Washington. Diatoms were analyzed at 1-cm intervals downcore at two sites (44 and 11) in the Briscoe Lake transect of the Long Beach locality (fig. 6) to establish marine surge origins of target tsunami deposits. A scan of the upper 25 cm of core 44 indicated one horizon of elevated marine diatom abundance at 25 cm depth (fig. 10). This depth directly corresponds to a target tsunami sand layer and detritus cap, confirming the inferred marine inundation contact at 24–25 cm. Key marine species included *Amphora proteus*, *Paralia sulcata*, and *Thalassiosira paficia*. Freshwater assemblages of diatoms were dominated by *Eunotia pectinal*, *Pinnularia viridis*, *Gomphonema parvulum*, *Gomphonema augustatum*, and *Navicula bacillum*.

Comparative analyses at site 11 indicated two horizons (9–10 and 35–40 cm depth) of elevated marine diatom abundance. The increased abundances of marine diatoms at these horizons correspond to logged detritus layers (upper horizon) and a combined sand layer with overlying detritus layer (lower horizon). A correlation analysis was performed on marine diatom abundance and logged detritus layers between 0 and 41 cm deep at site 11 to test the synchronicity of the two indicators at the 1-cm scale. The analysis yielded a correlation coefficient (R^2) of 0.7. Elevated concentrations of bromine were also used to establish marine surge origins for some detritus layers.

Bromine Marine Surge Tracer. Instrumental neutron activation analyses of sediments from Long Beach, Washington, show increases in bromine that are correlative to the increases in marine diatom abundance (fig. 10). Bromine concentrations measured throughout the length of core 44 from Long Beach, Washington, indicated a peak concentration (100 ppm) at a depth of 24–25 cm. This depth corresponds to a contact with an inferred tsunami-deposited detritus cap that also shows an increase in marine diatom abundance. These results highlight the possibility of using marine geochemical analytical techniques to map inundation extents where waning surge velocities can no longer entrain and deposit sand.

Radiocarbon Dating. Radiocarbon ages of the inferred tsunami sand layers or hosting deposits are shown in figure 11. Based on the calibrated dating results, the target tsunami ages appear to bracket the following ranges: 0–530 (core sites at Long Beach and Grayland), 735–975 (core sites at Grayland, Long Beach, and Neskowin), 920–1290 (Long Beach and Neskowin), and 1280–1410 cal. RYBP (Long Beach). Potential errors are associated with the dating of carbon material entrained and deposited by tsunamis. Marine surges entrain pre-event material from backshore drift, foredune soils, and bog peat surfaces, leading to dates that are potentially older than the tsunami event. In addition, a high radiocarbon production rate at about 300 yr ago typically yields radiocarbon dates that are about 100 yr younger than would be expected for that time period (Stuiver and Reimer 1993). With these potential dating errors in mind, the ranges of calibrated event dates appear to correspond to Cascadia earthquakes dated at 0.3, 1.1, and 1.3 Ka (Atwater et al. 2004). The remaining cluster of inferred tsunami dates (735–975 cal. RYBP) brackets an unidentified event at about 0.85 ± 0.15 Ka.

Discussion

Distances of Paleotsunami Inundation. *Neskowin, Oregon.* Detailed core logs from one represen-

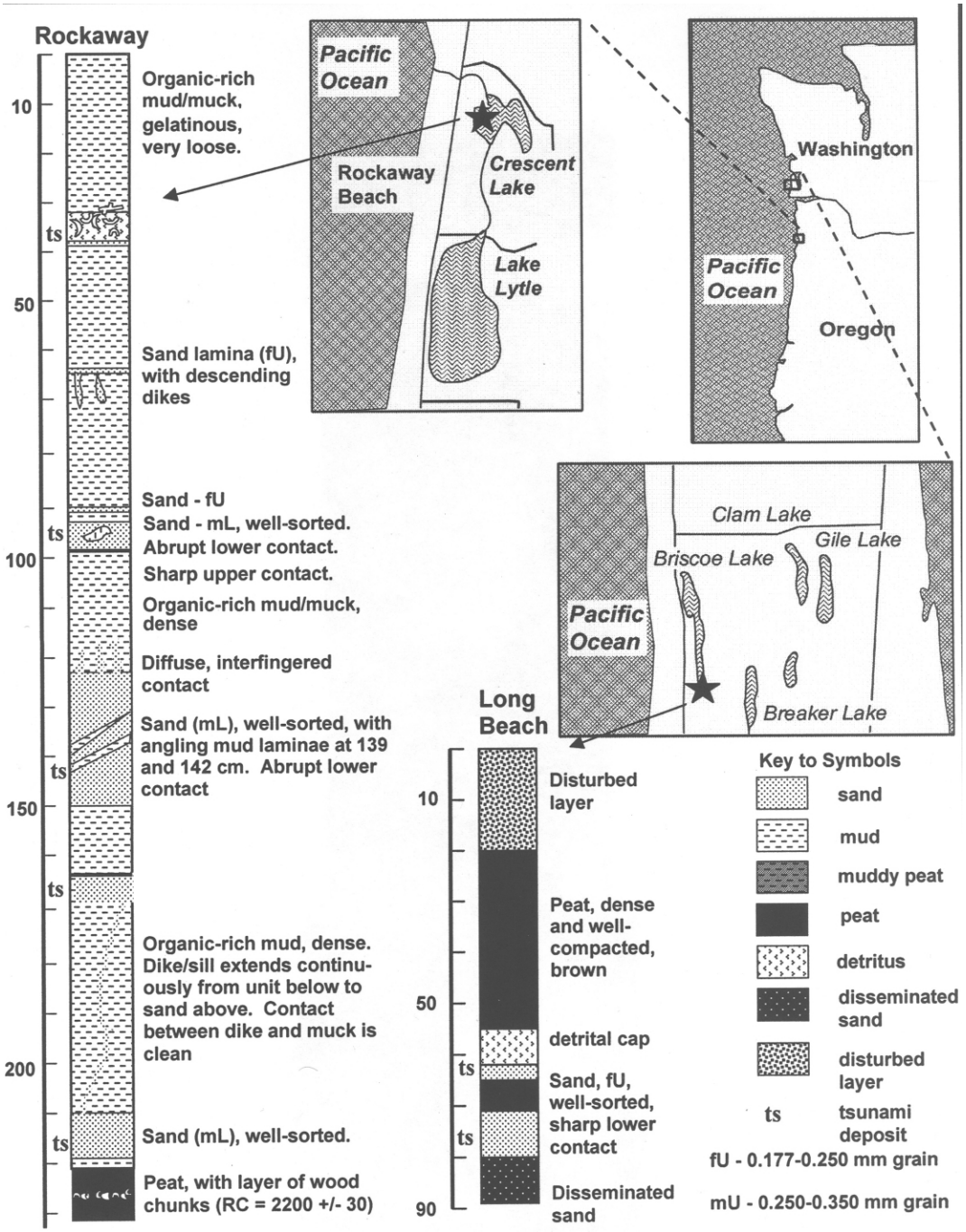

Figure 8. Examples with detailed descriptions of representative cores that were analyzed from the various field localities. *RC* = radiocarbon years before present; *fU* = well sorted sand clasts corresponding to "upper-fine" grain size (0.177–0.250 mm); *mL* = well sorted sand clasts corresponding to "lower-medium" grain size (0.250–0.350 mm). Vertical scale is in centimeters below sediment surface.

tative transect at the southernmost locality, Neskowin, are shown in figure 4. Two proximal cores (sites 153 and 141) contain a distinct paleotsunami sand layer at about 30 cm depth. A sample of peat extracted from above this layer in core 153 returned a modern radiocarbon date. This uppermost paleotsunami deposit corresponds to the 1700 Cascadia earthquake. It extends a maximum

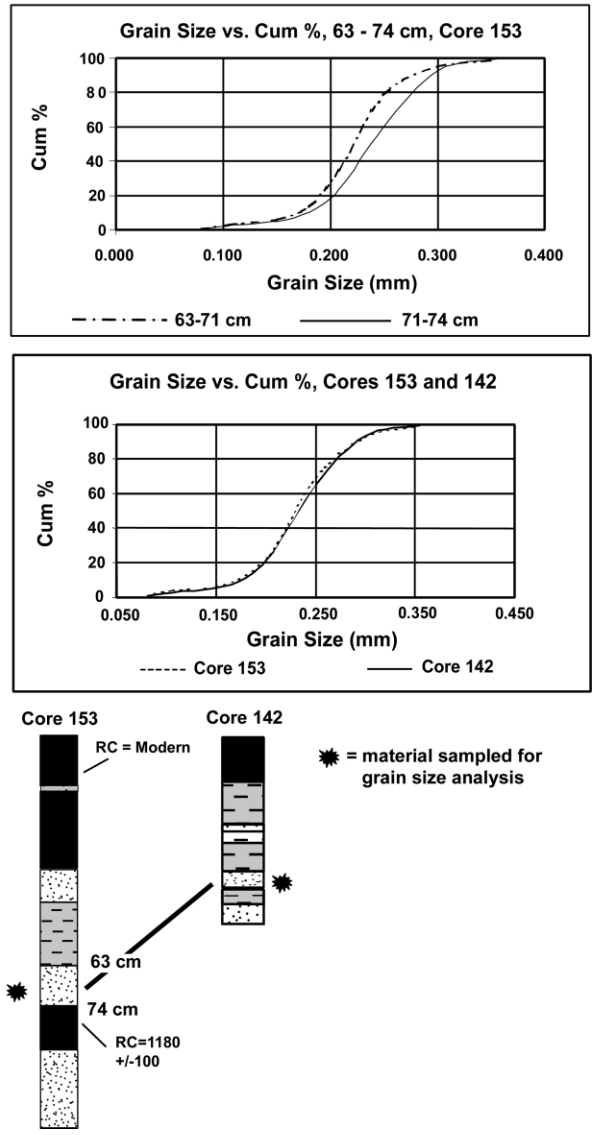

Figure 9. Sediment size analysis of the tsunami-deposited sand layers showed that thick tsunami layers (>3 cm) fined upsection. Sieving did not show a landward-fining trend of deposited sand. The upper plot corresponds to the sand layer from core 153 that has been divided into a lower section (71–74 cm) and an upper section (63–71 cm) for comparative analysis. The lower plot corresponds to grain size analysis for all of the sand from 63–74 cm in core 153 and all of the sand from the layer shown in core 142. *RC* = radiocarbon years before present.

distance of 0.3 km from the present shoreline. Two additional paleotsunami sand layers at site 153 overlie a peat sample that was dated at 920–1290 cal. RYBP. These two paleotsunami sand sheets extend 600 m inland in the northern marsh transect (fig. 4). Additional core transects at Neskowin indicated a fourth paleotsunami sand sheet at a depth that was traced 1.5 km inland from the modern shoreline. This oldest paleotsunami deposit from Neskowin predates the central marsh peat (920–1290 cal. RYBP) and is assigned to the next-oldest Cascadia earthquake, dated at 1.3 Ka (Atwater et al. 2004). The shoreline at Neskowin is thought to have remained at its present position for the last 2 Ka based on dated beach deposits (Hart and Peterson 1997).

Rockaway, Oregon. A core transect from Rockaway, Oregon, is shown in figure 5. The south-north directed cores (cores 91–94) include a sand layer that is easily correlated in all of the cores. A sample of peat underlying one of these sand layers dated at 735–795 cal. RYBP. The west-east directed transect included a thin sand layer in the first two proximal cores (cores 108 and 109). This tsunami layer corresponds to the 1700 Cascadia earthquake and extends a maximum distance of 0.4 km from the present shoreline. These cores included a thicker sand layer at a depth that was continuous in the remaining cores (cores 110–113). A sample of peat from beneath this sand sheet in core 112 was dated at 840–975 cal. RYBP.

The Rockaway core in figure 8 is representative of the record found in both Lake Lytle and Crescent Lake, where an additional 16 cores were extracted. This core includes a tsunami deposit corresponding to the 1700 Cascadia earthquake. A wood twig sampled from above a sand layer at a depth of 2 m below the sediment surface indicated a date of 2000–2325 cal. RYBP. Seven distinct sand layers were logged between the uppermost and lowest sand layers in this core. Further coring in these lakes will enable correlation of these sand layers to the regional paleoseismicity record.

Long Beach Peninsula, Washington. Three paleotsunami events are recorded in cores from the Briscoe Lake transect of the Long Beach locality (fig. 6). The youngest paleotsunami is identified by a sand layer at site 44 but by only a detritus layer at site 11. The detritus cap sampled from core 44 returned a radiocarbon age of 300–530 cal. RYBP, corresponding to the last Cascadia earthquake, in 1700. The maximum inland extent of sand (at site 44) represents a high-velocity inundation distance of 300 m from the 1700 beach retreat scarp (Woxell 1998), or ~0.5 km from the pre-event shoreline (Doyle 1996).

An older paleotsunami deposit (64 cm depth) at site 58 returned an age of 665–795 cal. RYBP (fig. 6). This sand layer is correlative to site 54, thereby extending the sand sheet to 700 m in west-east dis-

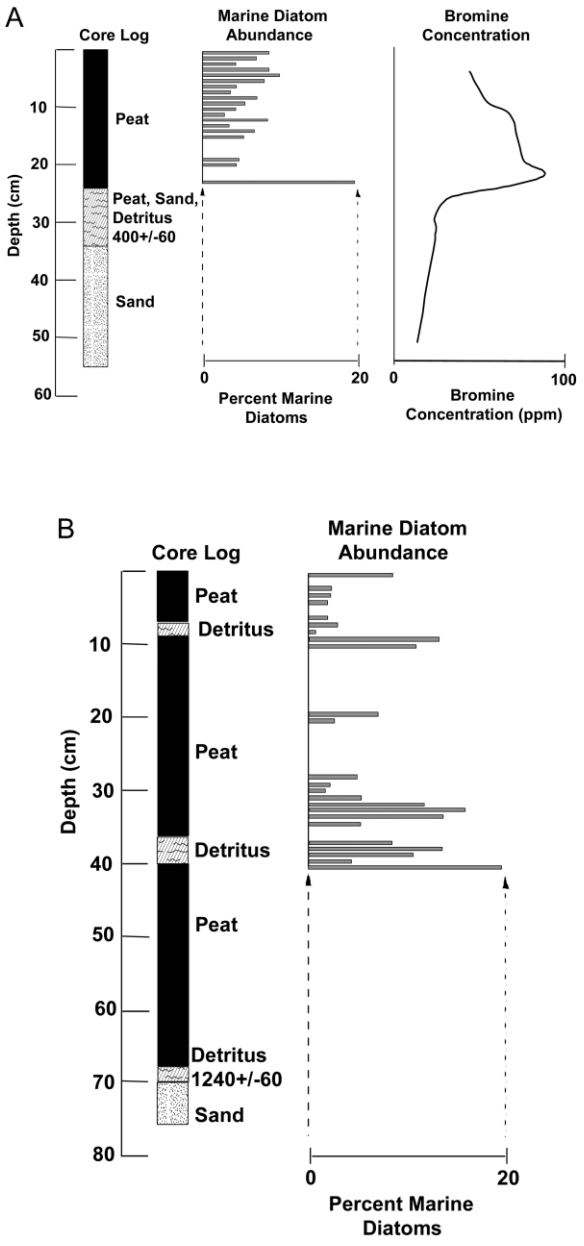

Figure 10. Tsunami layers in selected cores showed increased levels of marine tracers, including bromine and diatoms. *A*, Core was taken from site 44, Long Beach Peninsula; *B*, core was taken from site 11, Long Beach Peninsula (see fig. 6). Bromine concentration is in parts per million relative to whole sediment. Percent marine diatoms is percentage of all diatoms that are of marine origin.

tance, or at least 1000 m from a paleoshoreline position corresponding to the 0.8 ± 0.1 Ka period (fig. 12). A third paleotsunami sand sheet was observed in cores 11, 58, 59, 60, 61, 62, and 54. Radiocarbon dates of this event from sites 11 (990–1285 cal. RYBP) and 54 (1065–1320 cal. RYBP) indicate its origin from the Cascadia earthquake dated at 1.1 Ka. Both of the older paleotsunamis produced sand sheets that exceeded 1.0 km in inundation distance. A limiting age of the hosting peat (~1.2 Ka) precludes records of older paleotsunami sand sheets from the Long Beach locality.

Grayland Plains, Washington. Core logs from the Gould Road transect at the northernmost locality, Grayland Plains, are presented in figure 7. Sites 169, 170, and 172 host a paleotsunami deposit within 35 cm of the sediment surface. A date of 250 cal. RYBP for this paleotsunami event corresponds to the last Cascadia earthquake, in 1700. An older paleotsunami deposit was observed at 56 cm below the surface at site 172 and at similar depths at sites 171 and 173 (fig. 7). A stick sampled from the top of this sand layer at site 172 yielded an age of 655–880 cal. RYBP. Deeper paleotsunami sand deposits, preserved at sites 174 and 175, are close to the age of basal peat in the locality, ~1 Ka (Woxell 1998). This third paleotsunami corresponds to the Cascadia earthquake dated at 1.1 Ka (Atwater et al. 2004). The 1700 shoreline and 1.1-Ka shoreline were approximately 0.5 and 0.75 km landward from the modern shoreline, respectively (Woxell 1998). The two oldest paleotsunami sand sheets at sites 172, 173, 174, and 175 occur at least 1.0 km inland from corresponding paleoshorelines at 0.8 and 1.1 Ka (fig. 13).

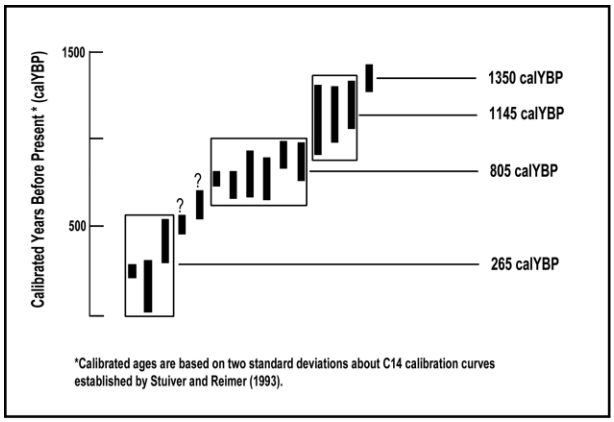

Figure 11. Results of radiocarbon dating of select horizons from all of the study sites presented in this article. Similar dates are enclosed in a box and have been averaged, as shown by the date to the right. Question marks indicate dates that do not fall within the various groupings. The 265, 1145, and 1350 cal. RYBP ages correlate to Cascadia subduction zone earthquakes as outlined in the literature (Darienzo and Peterson 1990; Atwater et al. 2004).

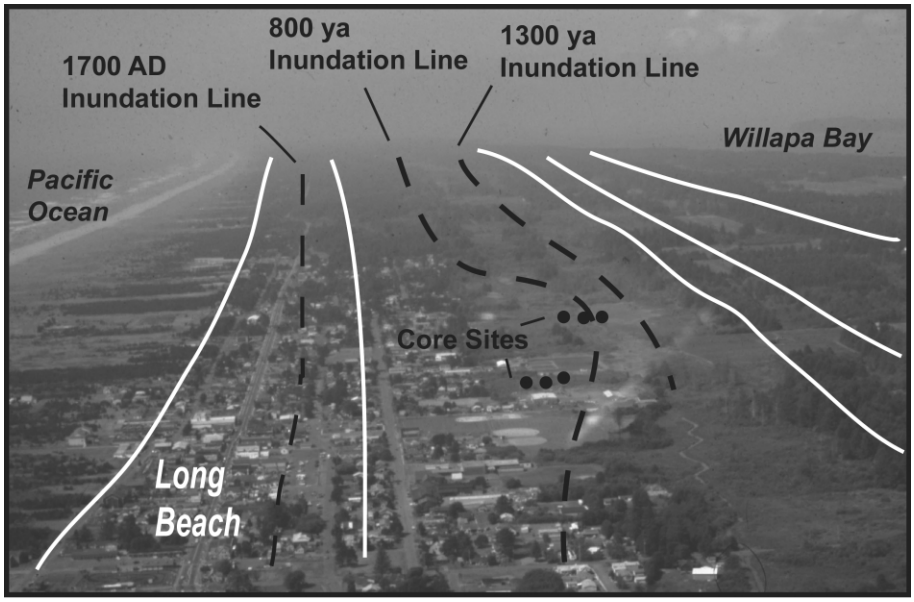

Figure 12. Estimated extent of paleotsunami inundation for the 1700 event, 0.8-Ka event, and 1.3-Ka event for Long Beach Peninsula. The maximum dune elevation, shown by white lines, is 8 ± 1 m. Dashed lines represent known distances based on correlation of sand layers in cores.

Unexpected Tsunami Magnitude. Three of the last four paleotsunami events yielded unexpected results, given the mapped surge inundation distances and corresponding earthquake parameters of magnitude and coseismic subsidence. For example, the last Cascadia earthquake, in 1700, resulted in 1–2 m of coseismic subsidence in southern Washington (Peterson et al. 2000). The magnitude of this earthquake has been estimated to be Mw ~9 (Satake et al. 1996). Nevertheless, the overland distance of sand inundation mapped for this event (~0.5 km) is less than half the distance of the preceding two or three paleotsunamis in the back-barrier settings of the central Cascadia margin.

The second-oldest paleotsunami demonstrates sand sheet inundation of at least 1.0 km inland distance over the 200-km-long study area. However, there is no record of coseismic subsidence in the study area associated with the age of this event (~0.8 Ka). The scale and continuity of inundation for this event in the central Cascadia margin argues against a far-field source from the Gulf of Alaska (Clague and Bobrowsky 1994) or Asian Pacific Ocean margins. For example, the far-field tsunami from the 1964 Gulf of Alaska subduction zone earthquake (Mw 9) left no record of overland inundation at any of the core sites in the four study localities. Additional work is needed to test for a near-field source of this event, such as from a rupture of the southern Cascadia margin and/or a continental slope landslide.

The oldest of the four paleotsunamis compared in this study of the central Cascadia margin is assigned to a Cascadia earthquake dated at 1.3 Ka (table 2). This event is associated with a minimum amount of subsidence (>0.5 m) in the southern Washington coast (Atwater 2000; Peterson et al. 2000; Atwater et al. 2004), yet it produced the maximum distance of sand sheet inundation, at least 1.5 km at the Neskowin locality (fig. 4). It is not known what rupture slip distributions or possible asperities might have contributed to the large run-up of the 1.3-Ka paleotsunami event.

Mapping Overland Paleotsunami Inundation. An important result of the tsunami deposit mapping in the beach plain localities was the recognition of robust records of paleotsunami inundation. Although sand sheet thickness varied widely (0.2–25 cm; table 3), the tsunami sand beds and laminae were easily identified and traced landward in peat and mud deposits. Eolian airfall deposits of sand in the bog peat were diffuse and lacked trace granule size fractions. Local difficulties with coseismic fluidization, such as sand blows and clastic sills (Fiedorowicz 1997), were overcome by dense coring strategies that traced target tsunami deposits out of liquefaction zones.

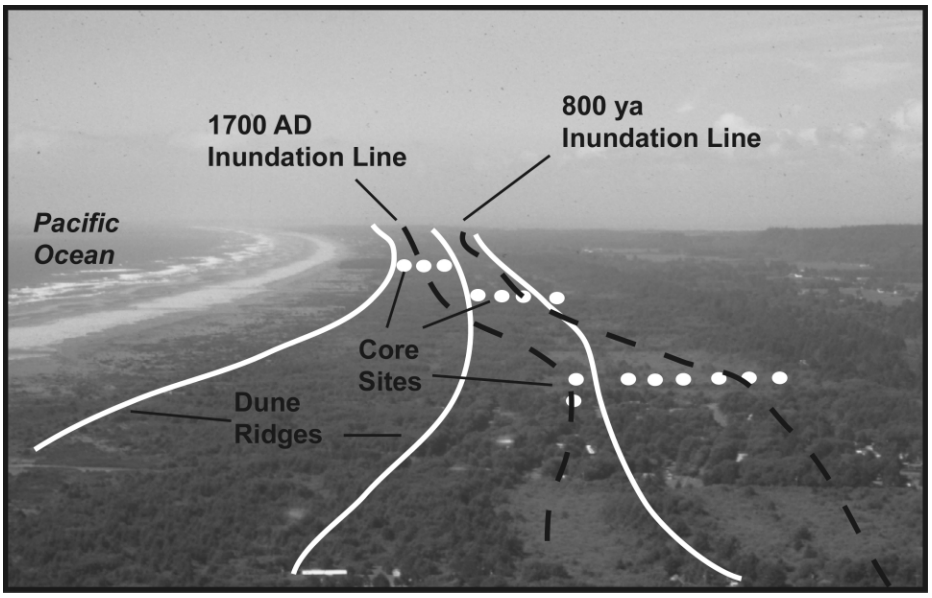

Figure 13. Inferred extent of paleotsunami inundation for the 1700 event and the 0.8-Ka event for the central Grayland Plains. The maximum dune elevation, shown by white lines, is 6 ± 1 m. Dashed lines represent known inundation distances based on the correlation of sand sheets.

The stratigraphic continuity of the sand sheet deposits (figs. 4–7) and the near omnipresence of debris capping layers proved to be important guides in tracing the tsunami inundation record. It is not known whether the termination of the sand sheet records resulted from decreasing flow velocities or dilution of suspended beach sand. Additional work is warranted to map low-velocity inundation further inland of the sand sheets, possibly using core records of debris caps and associated marine diatoms and/or bromine tracers.

The high-velocity inundation distances of 0.5–1.5 km reported here (table 3) are much greater, by factors of two to three, than those reported for coastal pond sites in the northernmost Cascadia margin (Hutchinson et al. 1997). However, similar distances of sand sheet deposition (1.0–1.5 km) are reported for somewhat channelized paleotsunami inundation from the southernmost Cascadia margin (Abramson 1998). In this report, we do not specifically address tsunami run-up height at the ocean shoreline. However, each of the study localities is fronted by forested foredunes of 6–10 m elevation above MSL. Efforts are underway to date the foredune ridges and establish their heights at the time of paleotsunami inundation.

Table 2. Occurrence Dates and Associated Subsidence for the Past Seven Cascadia Earthquakes

Event designation	Estimated age ± .1 Ka	Subsidence (m)
Y	1700 AD	~1
W	1100 cal. RYBP	?
U	1300 cal. RYBP	<.5
S	1700 cal. RYBP	~1
N	2500 cal. RYBP	<.5
L	2800 cal. RYBP	~1
J	3200 cal. RYBP	~1

Note. Taken from Atwater et al. 2004.

Conclusions

The results of this study indicate that there is a high preservation potential of tsunami-deposited sand sheets in back-barrier and beach plain settings. These sand sheets have been mapped and stratigraphically correlated to show continuity over hundreds of meters of landward-oriented lateral extent in bog and pond deposits. In addition, there is a significant correspondence between dated paleotsunami deposits from this study and frequently reported earthquake events (0.3, 1.1, and 1.3 Ka). This study also supports the occurrence of a tsunami event at ~0.8 Ka, originally reported from Vancouver Island. This event has not been broadly acknowledged in previous Cascadia paleoseismicity studies. Finally, landward extent of sand sheet deposition indicates high-velocity inundation dis-

Table 3. Summary of Inundation Extent of Prehistoric Tsunamis

Sand sheet location and event age	Sand sheet thickness range (cm)	Landward extent from current shoreline (km)	Current dune height (m)
Briscoe Lake, Long Beach:			
1700 AD	0–1	.8	8
.8 Ka	1–3	.8	8
1.3 Ka	1–4	1.4	8
Gould Road, Grayland:			
1700 AD	.2–5	1.5	6
.8 Ka	.3–9	1.7	6
Crescent Lake, Rockaway:			
1700 AD	.2–21	.5	6
.8 Ka	.2–24	.6	6
North Marsh, Neskowin:			
1700 AD	.2–11	.4	6
.8 Ka	.2–22	1.0	6
1.3 Ka	.2–13	1.0	6

Note. Distances as indicated are relative to modern shoreline position and dune elevation.

tances of 0.5–1.5 km in open-coast, low-elevation back-barrier vegetated settings.

ACKNOWLEDGMENTS

This research on paleotsunami inundation distances in the central Cascadia margin was funded by the National Oceanic and Atmospheric Administration (NOAA) Office of Sea Grant and Extramural Programs, U.S. Department of Commerce, under grant NA36RG0451, project R/CP-28, and by appropriations made by the Oregon State Legislature. Additional funding was provided by the Oregon Graduate Institute, through a grant from the Office of Naval Research, and by the Washington Department of Natural Resources through a grant from the NOAA Pacific Marine Environmental Laboratory Tsunami Modeling Center, Seattle, Washington.

REFERENCES CITED

Abramson, H. 1998. Evidence for tsunami and earthquakes during the last 3500 years from Lagoon Creek, a coastal freshwater marsh, northern California. MS thesis, Humboldt State University, Arcata, CA, 75 p.

Atwater, B. F. 1987. Evidence for great Holocene earthquakes along the outer coast of Washington State. Science 236:242–244.

———. 1992. Geologic evidence for earthquakes during the past 2000 years along the Copalis River, southern coastal Washington. J. Geophys. Res. 97:1901–1919.

Atwater, B. F.; Nelson, A. R.; Clague, J. L.; Carver, G. A.; Yamaguchi, D. K.; Bobrowsky, P. T.; Bourgeois, J.; et al. 1995. Summary of coastal geologic evidence for past great earthquakes at the Cascadia Subduction Zone. Earthquake Spectra 11:1–18.

Atwater, B. F.; Tuttle, M. P.; Schweig, E. S.; Rubin, C. M.; Yamaguchi, D. K.; and Hemphill-Haley, E. 2004. Earthquake recurrence inferred from paleoseismology. *In* Gillespie, A. R.; Porter, S. C.; and Atwater, B. F., eds. The Quaternary period in the United States. Amsterdam, Elsevier, p. 331–350.

Clague, J. J., and Bobrowsky, P. Y. 1994. Tsunami deposits beneath tidal marshes on Vancouver Island, British Columbia. Geol. Soc. Am. Bull. 106:1293–1303.

Clague, J. J.; Hutchinson, I.; Mathewes, R. W.; and Patterson, R. T. 1999. Evidence for late Holocene tsunamis at Catala Lake, British Columbia. J. Coast. Res. 15:45–60.

Darienzo, M. E. 1987. Late Holocene geologic history of a Netarts salt marsh, northwest Oregon coast, and its relationship to relative sea level changes. MS thesis, University of Oregon, Eugene, 94 p.

Darienzo, M. E., and Peterson, C. D. 1990. Episodic tectonic subsidence of late Holocene salt marshes, northern Oregon central Cascadia Margin. Tectonics 9:1–22.

Doyle, D. L. 1996. Beach response to subsidence following a Cascadia subduction zone earthquake along the Washington-Oregon coast. MS thesis, Portland State University, Portland, OR, 113 p.

Duce, R. A.; Winchester, J. W.; and Van Nahl, T. W. 1965. Iodine, bromine, and chlorine in the Hawaiian marine atmosphere. J. Geophys. Res. 70:1775–1799.

Fiedorowicz, B. 1997. Geologic evidence of historic and prehistoric tsunami inundation at Seaside, Oregon. MS thesis, Portland State University, Portland, OR, 197 p.

Folk, R. L. 1980. Petrology of sedimentary rocks. Austin, TX, Hemphill, 185 p.

Foster, I. D. L. 1991. High energy coastal sedimentary deposits: an evaluation of depositional processes in southwest England. Earth Surface Processes Landforms 16:341–356.

Fuge, R. 1988. Sources of halogens in the environment: influences on human and animal health. Environ. Geochem. Health 10:51–61.

Hart, R., and Peterson, C. 1997. Episodically buried forests in the Oregon surf zone. Oreg. Geol. 59:131–144.

Hemphill-Haley, E. 1996. Diatoms as an aid in identifying late-Holocene tsunami deposits. Holocene 6: 439–448.

Hutchinson, I.; Clague, J. J.; and Mathewes, R. W. 1997. Reconstructing the tsunami record on an emerging coast: a case study of Kanim Lake, Vancouver Island, British Columbia, Canada. J. Coast. Res. 13:545–554.

Jaffe, B., and Gelfenbaum, G. 1998. Sedimentation, erosion and flow in the July 17, Papua New Guinea tsunami. EOS: Trans. Am. Geophys. Union 79:F564.

Meyers, R. A.; Smith, D. G.; Jol, H. M.; and Peterson, C. D. 1996. Evidence for eight great earthquake-subsidence events detected with ground-penetrating radar, Willapa Barrier, Washington. Geology 24:99–102.

Minoura, K.; Shu, N.; and Uchida, M. 1994. Tsunami deposits in a lacustrine sequence of the Sanriku coast, northeast Japan. Sediment. Geol. 89:25–31.

Myers, E. P.; Baptista, A. M.; and Priest, G. R. 1999. Finite element modeling of potential Cascadia subduction zone tsunamis. Sci. Tsunami Hazards 17:3–18.

Nelson, A. R.; Kelsey, H. M.; Hemphill-Haley, E.; and Witter, R. C. 1996. A 7500-year lake record of Cascadia tsunamis in southern coastal Oregon. Geol. Soc. Am. Abstr. Progr. 28:5.

Peters, R.; Jaffe, B.; Peterson, C.; and Gelfenbaum, G. 2003. Cascadia tsunami deposit database. U.S. Geol. Surv. Open File Rep. 03-13, 24 p.

Peterson, C. D.; Doyle, D. L.; and Barnett, E. T. 2000. Coastal flooding and beach retreat from coseismic subsidence in the central Cascadia margin, USA. Environ. Eng. Geol. 6:255–269.

Peterson, C. D.; Gelfenbaum, G. R.; Jol, H. M.; Phipps, J. B.; Reckendorf, F.; Twichell, D. C.; Vanderburg, S.; and Woxell, L. 1999. *In* Great earthquakes, abundant sand, and high wave energy in the Columbia cell, USA. Coastal Sediments '99. Proc. Am. Soc. Civil Eng., p. 1676–1690.

Peterson, C. D., and Priest, G. R. 1995. Preliminary reconnaissance survey of Cascadia paleotsunami deposits in Yaquina Bay, Oregon. Oreg. Geol. 57:33–40.

Priest, G. R. 1995. Explanation of mapping methods and use of the tsunami hazard map of the Siletz Bay area, Lincoln County, Oregon. State of Oregon Department of Geology and Mineral Industries Open File Rep. O-95-05, 69 p.

Priest, G. R.; Myers, E.; Baptista, A.; Fleuck, P.; Wang, K.; and Peterson, C. D. 2000. Source simulation for tsunamis: lessons learned from fault rupture modeling of the Cascadia subduction zone, North America. Sci. Tsunami Hazards 18:77–106.

Satake, K.; Shimazaki, K.; Tsuji, Y.; and Ueda, K. 1996. Time and size of a giant earthquake in Cascadia inferred from Japanese tsunami record of January 1700. Nature 379:246–249.

Schlichting, R. 2000. Establishing the inundation distance and overtopping height of paleotsunami from the late-Holocene geologic record at open-coastal wetland sites, central Cascadia margin, USA. MS thesis, Portland State University, Portland, OR, 168 p.

Stuiver, M., and Reimer, P. J. 1993. Extended ^{14}C data base and revised CALIB 3.0 ^{14}C age calibration program. Radiocarbon 35:215–230.

Woxell, L. K. 1998. Prehistoric beach accretion rates and long-term response to sediment depletion in the Columbia River Littoral System, USA. MS thesis, Portland State University, Portland, OR, 143 p.